THE JOURNAL OF BIOLOGICAL CHEMISTRY VOL. 282, NO. 15, pp. 11238–11245, April 13, 2007

Calcium Influx and Mitochondrial Alterations at Synapses Exposed to Snake Neurotoxins or Their Phospholipid Hydrolysis Products*[S]

Received for publication, October 31, 2006, and in revised form, January 22, 2007 Published, JBC Papers in Press, February 20, 2007, DOI 10.1074/jbc.M610176200

Michela Rigoni[‡], Paola Pizzo[‡], Giampietro Schiavo[§], Anne E. Weston[§], Giancarlo Zatti[‡], Paola Caccin[‡], Ornella Rossetto[‡], Tullio Pozzan[‡¶], and Cesare Montecucco[‡1]

From the [‡]Department of Biomedical Sciences and Consiglio Nazionale Ricerche Institute of Neuroscience, University of Padova, 35121 Padova, Italy, [§]Cancer Research UK London Research Institute, Lincoln's Inn Fields Laboratories, London WC2A 3PX, United Kingdom, and [¶]Venetian Institute of Molecular Medicine, 35129 Padova, Italy

Snake presynaptic phospholipase A2 neurotoxins (SPANs) bind to the presynaptic membrane and hydrolyze phosphatidylcholine with generation of lysophosphatidylcholine (LysoPC) and fatty acid (FA). The LysoPC + FA mixture promotes membrane fusion, inducing the exocytosis of the ready-to-release synaptic vesicles. However, also the reserve pool of synaptic vesicles disappears from nerve terminals intoxicated with SPAN or LysoPC + FA. Here, we show that LysoPC + FA and SPANs cause a large influx of extracellular calcium into swollen nerve terminals, which accounts for the extensive synaptic vesicle release. This is paralleled by the change of morphology and the collapse of membrane potential of mitochondria within nerve bulges. These results complete the picture of events occurring at nerve terminals intoxicated by SPANs and define the LysoPC + FA lipid mixture as a novel and effective agonist of synaptic vesicle release.

Toxins in general, and neurotoxins in particular, are invaluable tools in the molecular analysis of specific cellular processes, from the activation of G protein-coupled receptors to the characterization of the events controlling regulated exocytosis (1). Much attention has been recently dedicated to a class of neurotoxins with phospholipase A2 (PLA2)[2] activity that are produced by different families of poisonous snakes (SPANs), whose precise biochemical and cellular mode of action has long remained elusive (2). A hallmark of their action *in vivo* and *in vitro* is the induction of enlargement of nerve terminals with large depletion of their content of synaptic vesicles (SV) (3–7).

We have recently shown that SPANs hydrolyze phospholipids of cultured neurons with generation of lysophosphatidylcholine (LysoPC) and fatty acids (FA) (8). This leads to a massive release of SV, with their incorporation into the presynaptic plasma membrane and consequent surface exposure of SV luminal epitopes (8–10). These and other experiments performed with models of SNARE-mediated membrane fusion provided evidence for the involvement of hemifusion lipid intermediates in exocytosis (11–17). The presence of LysoPC on the external leaflet of the presynaptic plasma membrane and of FA on both sides, caused by SPANs or by the addition of LysoPC and FA mixture (LysoPC + FA), promotes the formation of the hemifusion intermediate and its transition to an open pore. At the same time, this change in lipid composition of the membrane inhibits the reverse process (*i.e.* the fission and retrieval of SV). A balanced SV exocytosis-endocytosis cycle is at the basis of synaptic transmission at nerve terminals (18–20). SPANs promote exocytosis and inhibit endocytosis and, therefore, disrupt this finely tuned balance, causing the fusion of SV and formation of nerve terminal bulges decorated with the luminal domain(s) of SV proteins on their surface (9, 10). EM analysis reveals that nerve terminals are almost completely depleted of SV, with disappearance of both the "ready-releasable" pool and of the much larger "reserve" SV pool (3–8). Whereas depletion of the already docked SV was expected (16), more surprising is the depletion of the "reserve" SV pool (21), since the membrane changes induced by LysoPC + FA are predicted to act predominantly on SV bound to the presynaptic membrane or which can rapidly enter in contact with its cytosolic leaflet. These SV have been defined as rapidly releasable vesicles, to be distinguished from the reserve pool of vesicles whose release is caused by the rise of the nerve terminal cytosolic Ca^{2+} concentration, which follows an extensive stimulation (21–23).

Here we have investigated the mechanism by which SPANs and the LysoPC + FA lipid mixture cause a massive SV release. Using primary cultures of different types of neurons, we found that the synaptic bulging induced by SPANs and LysoPC + FA is followed by a sustained increase in $[Ca^{2+}]_i$. At the same time, the mitochondrial membrane potential collapses. Upon SPAN or lipid mixture incubation, mitochondria change shape and appear to accumulate within bulges characterized by high calcium. Based on these findings, we present here a general model of nerve terminal blockade induced by SPANs or by the LysoPC +

* This work was supported by grants from Telethon-Italia GGP06133, the University of Padova, FIRBRBNE01RHZM, and Cancer Research UK. The costs of publication of this article were defrayed in part by the payment of page charges. This article must therefore be hereby marked "*advertisement*" in accordance with 18 U.S.C. Section 1734 solely to indicate this fact.

[S] The on-line version of this article (available at http://www.jbc.org) contains supplemental Figs. S1 and S2 and Movies 1 and 2.

[1] To whom correspondence should be addressed: Dept. of Biomedical Sciences, University of Padova, Viale G. Colombo, 3, 35121 Padova, Italy. Tel.: 39-0498276058; Fax: 39-0498276049; E-mail: cesare.montecucco@unipd.it.

[2] The abbreviations used are: PLA2, phospholipase A2; CGNs, cerebellar granule neurons; EM, electron microscopy; FA, fatty acid(s); LysoPC, lysophosphatidylcholine; mLysoPC, 1-myristoyl-lysophosphatidylcholine; OA, oleic acid; SCMN, spinal cord motor neuron; SPAN, snake presynaptic phospholipase A2 neurotoxin; SV, synaptic vesicle(s); TMRE, tetramethylrhodamine methyl ester; VDCC, voltage-gated Ca^{2+} channel.

FA mixture that explains the release of both the recycling and the reserve pools of SV.

EXPERIMENTAL PROCEDURES

Cell Cultures—Rat cerebellar granular neurons (CGNs) were prepared from 6-day-old Wistar rats as previously described (9, 24) and used 6–8 days after plating. Primary rat spinal motor neurons (SCMNs) were isolated from Sprague-Dawley (embryonic day 14) rat embryos and cultured following previously described protocols (25, 26). All experiments were performed using SCMNs differentiated for 5–8 days *in vitro*.

Fura2-AM Loading and Image Acquisition—Neurons grown on 24 mm coverslips were incubated in complete medium with 3 μM Fura-2/AM and 0.02% pluronic (Molecular Probes, Inc., Eugene, OR) for 30 min at 37 °C and then washed. To prevent Fura-2 leakage and sequestration, 250 μM sulfinpyrazone (Sigma) was present throughout the loading procedure and $[Ca^{2+}]_i$ measurements. After loading, cells were bathed in Krebs-Ringer buffer (KRH, in the case of CGNs) or E4 medium (Extra-4, in the case of SCMNs). KRH composition was as follows: 125 mM NaCl, 5 mM KCl, 1.2 mM $MgSO_4$, 2 mM $CaCl_2$, 1.2 mM KH_2PO_4, 6 mM glucose, and 25 mM HEPES, pH 7.4. E4 composition was as follows: 120 mM NaCl, 3 mM KCl, 2 mM $MgSO_4$, 2 mM $CaCl_2$, 10 mM glucose, and 10 mM HEPES, pH 7.4. Coverslips were mounted on a thermostated chamber (Medical System Corp.), placed on the stage of an inverted epifluorescence microscope (Axiovert 100 TV; Zeiss), equipped for single cell fluorescence measurements and imaging analysis (27). Samples were alternatively illuminated at 340 and 380 nm (every 15 s for 20–30 min after SPAN addition and every 10 s for 15–20 min after lipid exposure) through a ×40 oil immersion objective (numerical aperture 1.30; Zeiss), exposure times of 100 ms. Data were analyzed with MATLAB™ (The MathWorks, Natick, MA) and ImageJ version 1.35.

Lipid Mixture Preparation, Neurotoxins, and Inhibitors—1-Myristoyl-lysophosphatidylcholine (mLysoPC; Sigma) and oleic acid (OA; Sigma) mixture (mLysoPC + OA) was prepared as previously described (8). Notexin, taipoxin, and textilotoxin were purchased from Venom Supplies; β-bungarotoxin was from Sigma. Their purity was controlled by SDS-PAGE, and their PLA2 activity was measured with the Cayman secretory PLA2 assay kit. ω-Conotoxin MVIIC was from Latoxan, and nimodipine was from Tocris. Ionomycin and monensin were purchased from Calbiochem.

Mitochondrial Imaging—SCMNs or CGNs were loaded with tetramethylrhodamine methyl ester (TMRE) (10 nM; Molecular Probes) in medium supplemented with the multidrug resistance pump inhibitor CsH (1.6 μM final concentration) (28) for 30 min at 37 °C. Fluorescence images were acquired with a Leica AD MIRE3 inverted microscope, equipped with a Leica DC500 CCD camera, ×63 oil immersion objective (NA 1.4), using an exposure time of 50 ms. Data were collected using Leica FW4000 software and analyzed with Leica Deblur and ImageJ version 1.35. The average fluorescence of isolated mitochondria exposed to SPANs or the lipid mixture was recorded as a function of time. Intensity variations were expressed as a percentage of the initial value. Data represent the average of at least five regions of interest. For morphological staining of mitochondria, CGNs were incubated with 300 nM Mitotracker Red (Molecular Probes) for 15 min at 37 °C and then washed; images were acquired as above.

Measurement of Cellular ATP—CGNs (300,000/13-mm coverslip) were transfected at 5 days *in vitro* with cytosolic luciferase with a standard Lipofectamine™2000 procedure, using 1.5 μg of DNA. Measurements of cell luminescence were performed 24 h after transfection in cells pretreated or not with 25 nM taipoxin or the mLysoPC + OA lipid mixture (25 μM for 15 min; $n = 4$ for each condition) as described (29). Cells were constantly perfused with a modified Krebs-Ringer buffer (mKRB: 125 mM NaCl, 5 mM KCl, 1 mM Na_3PO_4, 1 mM $MgCl_2$, 1 mM $CaCl_2$, 20 mM HEPES, 5.5 mM glucose, pH 7.4, at 37 °C) with 20 μM luciferin. Complete equilibration in the chamber with the new medium was obtained in 5 s. Under these conditions, the light output of a coverslip of transfected cells was in the range of 5,000–10,000 counts/s *versus* a background lower than 100 counts/s.

In addition, the cellular ATP content was determined in CGNs, plated in a Petri dish (2×10^6 cells), at 7 days *in vitro* by a luciferin luciferase assay (ATP Bioluminescent Assay kit CLS II; Roche Applied Science) with an LKB Wallac 1250 luminometer. After treatment (mKRB, 25 μM lipid mixture for 15 min or 25 nM taipoxin for 60 min), cells were diluted in Tyrode buffer medium (145 mM NaCl, 5 mM KCl, 1 mM $MgCl_2$, 0.5 mM NaH_2PO_4, 5 mM glucose, 15 mM Hepes, pH 7.7), and ATP was extracted by adding 0.3 M perchloroacetic acid. Samples were kept on ice for 5 min and centrifuged at 18,000 × *g* for 10 min. The pH of the supernatant was adjusted to 7.7 ± 0.1 with a buffer solution of $KHCO_3$ (1 M) and KOH (1 M); the suspension was centrifuged at 18,000 × *g* for 5 min, and the supernatant was used for the analysis. The ATP content of each sample was estimated using the internal standard method in which 25 pmol of ATP were added twice to the assay. Analysis was repeated on triplicates for each condition. In both procedures for ATP content assay, the number of cells analyzed in each condition was equal, as determined by protein concentration measurement.

Electron Microscopy—CGNs were plated onto 13-mm polylysin-coated Thermanox coverslips (Nunc) and, after 6 days in culture, exposed to either SPANs (6 nM for 1 h) or mLysoPC + OA (25 μM for 15 min). Samples were then fixed for 1 h at room temperature in 2.5% glutaraldeyde (EM grade; Applichem) in phosphate buffer. Cells were then washed repeatedly with phosphate buffer and subjected to secondary fixation with 1% osmium tetroxide for 30 min, followed by extensive washes. Samples were then dehydrated with ascending grades of ethanol, araldite-embebbed for 2 days, and stained with aqueous uranyl acetate and lead citrate. Sections were imaged in a Jeol 1010 electron microscope equipped with a 2,000 × 2,000-pixel digital camera (GATAN).

RESULTS

Cytosolic $[Ca^{2+}]_i$ Increases in Nerve Terminals Exposed to Snake Presynaptic PLA2 Neurotoxins—A rise in intrasynaptic Ca^{2+}, such as that caused by prolonged nerve stimulation, is known to trigger SV mobilization from the reserve pool (21–23). We thus hypothesized that the extensive SPAN-induced

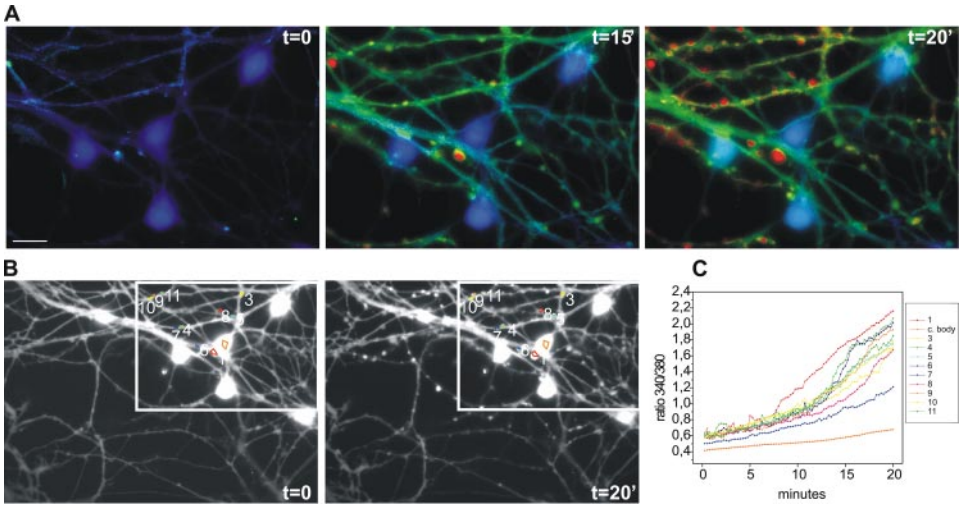

FIGURE 1. **$[Ca^{2+}]_i$ increase induced by taipoxin in cultured neurons.** *A*, three pseudocolor images from a movie of CGNs loaded with Fura2-AM and treated with 25 nM taipoxin for 20 min (the complete video is provided in supplemental materials as Movie 1). $[Ca^{2+}]_i$ increase, from *blue* (low $[Ca^{2+}]_i$) to *red* (high $[Ca^{2+}]_i$), specifically occurs within membrane bulges, whereas cell bodies remain largely unaffected. Similar results were obtained with notexin, textilotoxin, and β-bungarotoxin. *Scale bar*, 10 μm. *B*, fluorescent images from the experiment in *A* at $t = 0$ and after 20 min of treatment. The *white box* corresponds to the area shown in *pseudocolors* in *A*, whereas the *numbered* and *colored area* selections indicate the regions of interest whose time courses of changes in 340/380 fluorescence ratios are reported in *C*. This experiment is representative of many performed with different neurotoxins, and always several different nerve bulges were tracked at the same time.

release of SV, leading to a complete impairment of the nerve terminal, could indeed be caused by a rise in $[Ca^{2+}]_i$. To test this possibility, we have used primary cultures of rat cerebellar granular cells and spinal cord motor neurons. Cells were loaded with the intracellular calcium indicator Fura-2 and then treated with either SPANs or LysoPC + FA mixture. Fig. 1*A* shows three video images of Fura-2 loaded CGNs taken at different time points after application of 25 nM taipoxin, a SPAN isolated from the venom of *Oxyuranus scutellatus scutellatus*. The images are pseudocolor-coded and report the ratio of the probe emission intensity at 510 nm following alternative excitation at 340 and 380 nm. The 340/380 ratio is a function of the intracellular Ca^{2+} concentration ($[Ca^{2+}]_i$), whereby an increase in $[Ca^{2+}]_i$ is encoded as a shift of the pseudocolors from *blue* to *red* (video provided as supplemental Movie 1). A significant increase of the 340/380 ratio was observed in the bulges already at 10 min after toxin application, and the rise continued with time. In contrast, $[Ca^{2+}]_i$ was unchanged in cell bodies. This selected localization of the Ca^{2+} rise is likely to result from the specific binding, and therefore action, of the toxin at nerve terminals. The larger surface to volume ratio of nerve terminals compared with the cell body is also to be considered (see below). Fig. 1*C* shows a quantitative analysis of the 340/380 fluorescence ratio changes measured at the level of different bulges and a cell body (Fig. 1*B*) as a function of time. Individual bulges differ significantly in their rate of $[Ca^{2+}]_i$ rise, but the overall trend is similar. Very similar results were obtained in SCMNs and with structurally different snake PLA2 neurotoxins (*i.e.* notexin, β-bungarotoxin, and textilotoxin (not shown)), indicating that the results obtained here are not restricted to a single neuronal subtype or to the SPAN used. Incubation with control medium did not alter the level and distribution of intracellular Ca^{2+} (Fig. S1 and supplemental Movie 2).

Lysophosphatidylcholine/Fatty Acid Mixture Causes an Increase in $[Ca^{2+}]_i$ in Cultured Neurons—A similar result was obtained when CGNs were treated with the LysoPC + FA lipid mixture (Fig. 2*A*). Again, $[Ca^{2+}]_i$ increased with time within the bulges induced by the lipid mixture, but in this case a rise was also detected at the level of cell bodies (*black trace*). The complete time course of the increase in $[Ca^{2+}]_i$ in different bulges and in a cell body is shown in Fig. 2*C*. The ability of the lipid mixture to increase $[Ca^{2+}]_i$ both at the level of bulges and cell bodies, compared with the restricted action of SPANs on neurites, was expected on the basis of the fact that LysoPC and FA can partition into the plasma membrane at any site, whereas SPANs bind specifically to the presynaptic membrane of nerve terminals (2, 30). On the other hand, the larger $[Ca^{2+}]_i$ increase in the presynaptic regions compared with the cell body could also be influenced by the different surface/volume ratio of the two compartments. Any modification of the homeostatic mechanisms controlling Ca^{2+} at the plasma membrane is expected to cause substantial variations in the tiny cytosolic rim of the presynaptic membrane, whereas the same modification should take longer to affect the bulk $[Ca^{2+}]_i$ in the cell body.

Supplemental Fig. S2 shows that the component of the LysoPC + FA lipid mixture most effective in raising the intracellular Ca^{2+} concentration is LysoPC and that FA, when added alone, had no effect. However, the two molecules clearly synergize in order to produce the effect shown by the mixture in Fig. 2*C* and in supplemental Fig. 2*A*. This finding parallels the neuroparalytic effects that the lipid mixture and the two lipids alone have on the neuromuscular junction of the hemidiaphragm preparation (8).

Mechanisms of $[Ca^{2+}]_i$ Increase inside Nerve Terminals Poisoned with Lysophosphatidylcholine/Fatty Acid Mixtures—These findings rise the question as to whether the Ca^{2+} increase triggered by the toxins or by the lipid mixture derives from Ca^{2+} influx from the extracellular medium or depends on Ca^{2+} mobilization from intracellular stores, or both. To address this question, the experiments shown in Fig. 2 were repeated in CGNs incubated with medium without $CaCl_2$ and supplemented with 150 μM EGTA (Ca^{2+}-free buffer) (Fig. 3*B*). SPANs could not be used in these tests as Ca^{2+} is strictly required for their phospholipase activity (2). Under these conditions, the lipid mixture caused a very small Ca^{2+} rise and at very late time points (Fig. 3, compare *A* and *B*). This Ca^{2+} increase is small and must derive from intracellular stores. In order to distinguish in our primary neuronal culture the different Ca^{2+}-containing compartments on the basis of their luminal pH, we used

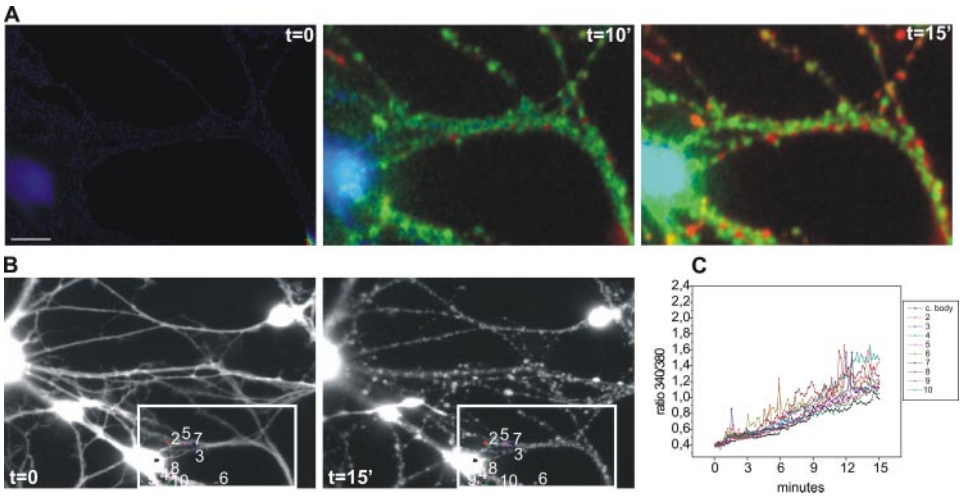

FIGURE 2. **Increase of $[Ca^{2+}]_i$ induced by an equimolar mixture of lysophosphatidylcholine and oleic acid (mLysoPC + OA) in cultured neurons.** *A*, three *pseudocolor images* from a movie of CGNs loaded with Fura2-AM and treated with 25 μM mLysoPC + OA for 15 min. At variance from SPAN-treated neurons, $[Ca^{2+}]_i$ appears to increase also in the cell body, although its increase is lower than within nerve bulges. *Scale bar*, 10 μm. *B*, fluorescent images from the experiment in *A* at $t = 0$ and at $t = 15$ min. *C*, analysis of the 340/380 fluorescence ratio of the selected *boxed region* as a function of time. Each trace shows the ratio changes of individual regions of interest. The phenomenon was highly reproducible in many experiments performed with different neuron preparations, and the one shown here is very representative of the ensemble.

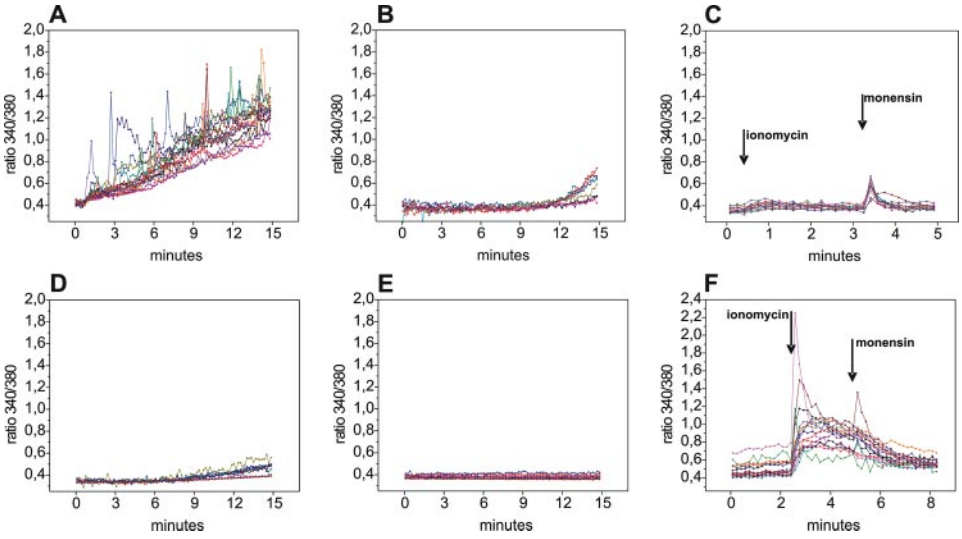

FIGURE 3. **Origin of $[Ca^{2+}]_i$ increase within synaptic bulges induced by mLysoPC + OA.** CGNs were exposed to 25 μM mLysoPC + OA for 15 min in the presence (*A*) or absence (*B*) of extracellular Ca^{2+} (Ca^{2+}-free buffer: KRH without $CaCl_2$ + EGTA 150 μM). *C*, control neurons were sequentially exposed to ionomycin and monensin (1 and 5 μM, respectively) in Ca^{2+}-free buffer to determine the increase in $[Ca^{2+}]_i$ contributed by the emptying of internal Ca^{2+} stores. *D*, cells were pretreated with 1 μM ionomycin (final concentration) in Ca^{2+}-free buffer and then incubated with 25 μM mLysoPC + OA for 15 min in the same medium, whereas in *E*, cells were pretreated with monensin (5 μM, final concentration) in addition to ionomycin in Ca^{2+}-free buffer and then exposed to the lipid mixture. Lipid mixture was added at $t = 0$. *F*, the result of the same experiment performed in *C* on cells pretreated with 25 μM mLysoPC + OA for 15 min in Ca^{2+}-free buffer. These traces refer to experiments performed on the same cell culture and are representative of three different sets of experiments.

a simple procedure (31). Cells were first treated with ionomycin in Ca^{2+}-free buffer. This Ca^{2+} ionophore exchanges Ca^{2+} for $2H^+$ and can very effectively release the cation but only from organelles with neutral/alkaline pH lumena (primarily ER, mitochondria) (32). A very small and transient rise in $[Ca^{2+}]_i$ was observed in control cells under these conditions (Fig. 3*C*). The acidic pH of other organelles (Golgi, secretory vesicles, and lysosomes) was then collapsed by the addition of monensin, and this induced a much larger increase in $[Ca^{2+}]_i$, indicating that most Ca^{2+} stores in these cells have an acidic luminal pH (Fig. 3*C*). Monensin was ineffective without ionomycin (not shown). The experiments presented in Fig. 3, *D* and *E*, demonstrate that the residual late rise of $[Ca^{2+}]_i$ shown in Fig. 3*B* derives mainly from intracellular acidic compartments. Indeed, in the experiments presented in Fig. 3*D*, neurons were first preincubated with 1 μM ionomycin in Ca^{2+}-free buffer and then exposed to 25 μM mLysoPC + OA. Under these conditions, the lipid mixture still elicited a late Ca^{2+} rise, indicating that it acted on stores insensitive to ionomycin. A complete suppression of the Ca^{2+} rise by mLysoPC + OA was achieved by the concomitant pretreatment with ionomycin and monensin (Fig. 3*E*).

Last, but not least, it should be noted that neurons exposed to the lipid mixture in Ca^{2+}-free buffer showed a higher response to ionomycin with respect to control neurons, and most bulges did not respond at all to monensin (Fig. 3, compare *F* with *C*). This latter observation suggests that, following exposure to the lipid mixture, there is an intracellular partition of fatty acids, which are known to act similarly to monensin and to quench transmembrane proton gradients (33). Intracellular acidic compartments, that under normal conditions cannot be emptied by ionomycin, become thus available to its action. Indeed, the same result was obtained when neurons were pretreated in Ca^{2+}-free buffer with the protonophore carbonylcyanide *p*-trifluoromethoxyphenyl hydrazone, a well known quencher of transmembrane pH gradients (not shown).

In order to investigate the nature of Ca^{2+} influx through the plasma membrane, neurons were incubated with the P/Q and N-type voltage-gated Ca^{2+} channel (VDCC) inhibitor ω-conotoxin MVIIC and with the L-channel inhibitor nimodipine. This treatment did not prevent the rise of $[Ca^{2+}]_i$ caused by the lipid mixture, although a very small reduction in the rate of the Ca^{2+} increase was observed in some neurons treated with these VDCC inhibitors (Fig. 4, compare *A* and *B*). Using isolated neuromuscular junction preparations, whose VDCCs are well characterized

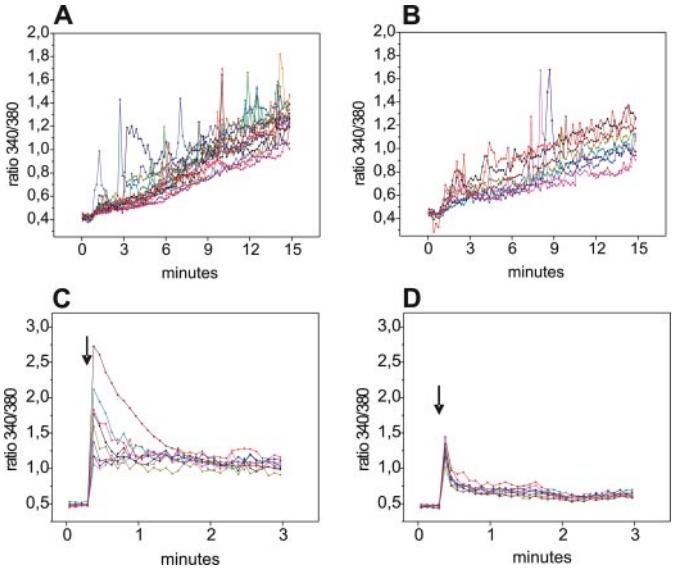

FIGURE 4. **Mode of Ca^{2+} influx inside nerve terminals exposed to mLysoPC + OA.** CGNs were exposed to 25 μM mLysoPC + OA for 15 min in the absence (*A*), or in the presence (*B*) of the Ca^{2+} channel blockers ω-conotoxin MVIIC (3 μM) and nimodipine (1 μM). $[Ca^{2+}]_i$ increase in control neurons following membrane depolarization induced by KCl (55 mM final concentration, *arrows*) in the absence (*C*) or presence (*D*) of the same Ca^{2+} channel blockers as in *B*. Each trace shows the ratio changes of individual regions of interest. Representative traces from one set of experiments of three are presented.

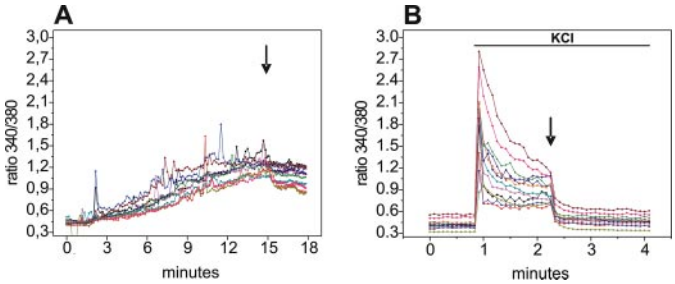

FIGURE 5. **Efflux of Ca^{2+} from nerve terminals treated with mLysoPC + OA.** *A*, CGNs were exposed to 25 μM mLysoPC + OA for 15 min in KRH buffer, and then EGTA (3 mM final concentration) was added (*arrow*). *B*, nerve terminal $[Ca^{2+}]_i$ in control neurons was brought to levels close to those reached after a 15-min exposure to the lipid mixture by the addition of KCl (55 mM), and then extracellular Ca^{2+} was chelated by EGTA as in *A*. Each trace shows the ratio changes of individual areas, including nerve terminals. These traces are representative of three different sets of experiments.

and known to be effectively inhibited by ω-conotoxin MVIIC (34), we did not observe any change in the paralysis time induced by SPANs (not shown). Control experiments performed with neurons treated with these channel inhibitors and depolarized with 55 mM KCl showed about 50% reduction in the calcium influx (Fig. 4, compare *C* and *D*). Taken together, these results indicate that these synaptic VDCCs may contribute to the rise of $[Ca^{2+}]_i$ induced by SPANs in primary cultures of neurons but are clearly dispensable. One possible explanation is that LysoPC + OA induces in cultured neurons a nonspecific increase in the membrane permeability for small molecules, as it was shown to occur for cultured vascular smooth muscle and endothelial cells (35, 36) and in lymphoma cells (37). These leaks must be small or specific, since we detected no leakage of Fura-2 (756 Da) during treatment with SPANs or LysoPC + OA. Alternative possibilities are considered below.

Ca^{2+} Efflux Is Inhibited in Nerve Terminals Exposed to Lysophosphatidylcholine/Fatty Acid Mixtures—A sustained rise of $[Ca^{2+}]_i$ could additionally, or alternatively, be dependent on the impairment of the Ca^{2+} efflux mechanisms. Given that the steady-state $[Ca^{2+}]_i$ at rest is the result of the kinetic equilibrium between the rate of Ca^{2+} leak through the plasma membrane and the rate of Ca^{2+} efflux mediated by plasma membrane Ca^{2+} pumps and Na^+/Ca^{2+} exchangers, a reduction in the extrusion efficiency inevitably results in a rise of $[Ca^{2+}]_i$. In order to test this possibility, cells were incubated with the LysoPC + FA lipid mixture for 15 min, and then the extracellular Ca^{2+} was rapidly chelated by EGTA. The rate of $[Ca^{2+}]_i$ decrease, which is indicative of the rate of Ca^{2+} efflux, under these conditions was very slow and unable to bring the $[Ca^{2+}]_i$ to the resting level (Fig. 5*A*, *arrow*). At variance, in control cells where $[Ca^{2+}]_i$ was increased to similar levels by depolarization, the efflux rate was much higher as shown by the rapid return of $[Ca^{2+}]_i$ to basal level upon the addition of EGTA (Fig. 5*B*, *arrow*).

One possible cause of the inhibition of Ca^{2+} efflux in the presence of LysoPC + FA is a reduction of the cytosolic ATP by blockade of its mitochondrial synthesis (*e.g.* upon the addition of the membrane-permeable mitochondrial uncoupler carbonylcyanide *p*-trifluoromethoxyphenyl hydrazone). Interestingly, β-bungarotoxin is known to induce mitochondrial depolarization in brain synaptosomes, which in turn would result in an inhibition of ATP synthesis (38–40). We measured the ATP content of CGNs with two different methods: transfected luciferase in live neurons (29) and the traditional luciferin-luciferase assay performed on lysed cells. The first method indicates a reduction of 21% in ATP content in lipid mixture-treated cells compare with controls (6750 ± 440 *versus* 5350 ± 300, average counts/s ± S.E., n = 4) and of 20% in the case of taipoxin-treated cells (6850 ± 560 *versus* 5548 ± 400, average counts/s ± S.E., n = 4). With the luciferin-luciferase assay, a reduction of 34% in ATP content in both lipid mixture and taipoxin-treated cells was found with respect to controls (180 ± 9 pmol of ATP/10^6 control cells; 120 ± 2.4 pmol of ATP/10^6 lipid mixture-treated cells; 120 ± 11 pmol of ATP/10^6 taipoxin-treated cells; average value ± S.E., n = 3). A lower ATP decrease is detected by the luciferase transfection methods, because the intracellular luciferase response to ATP is nonlinear. Considering that neuronal projections and terminals are mainly affected by the SPANs and by the LysoPC + OA mixture (Figs. 1 and 2), these decreases indicate that the local decrease of the ATP concentration may be more dramatic.

Taken together, these findings suggest changes in mitochondrial function in nerve terminals poisoned by SPANs or treated with the LysoPC + OA lipid mixture.

Mitochondrial Changes Induced by Snake PLA2 Presynaptic Neurotoxins and Lysophosphatidylcholine/Fatty Acid Mixtures—We then analyzed the effects of SPANs and LysoPC + FA on single mitochondria in CGNs and SCMNs. Neurons were loaded with the potentiometric dye TMRE and then treated with SPANs or with the lipid mixture (Fig.

6). TMRE is accumulated within the mitochondrial matrix due to the negative membrane potential across the inner membrane of the organelles. Both treatments cause a progressive mitochondrial loss of dye, indicating that incubation of neurons with SPANs and LysoPC + FA results in a major reduction of the mitochondrial membrane potential (Fig. 6 and data not shown).

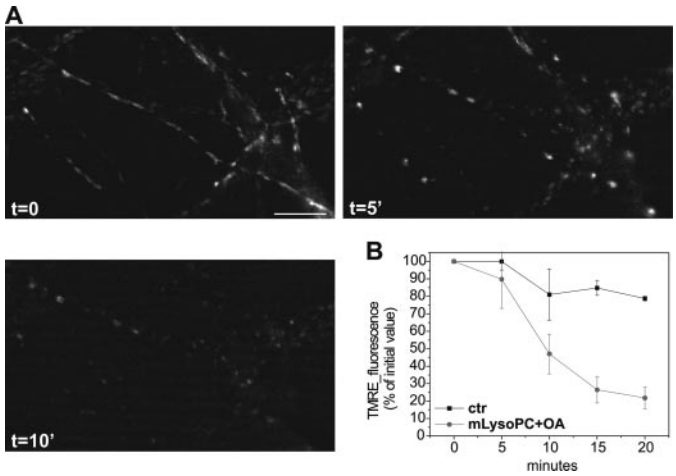

FIGURE 6. **Mitochondrial membrane potential changes in SCMNs treated with mLysoPC + OA.** *A*, fluorescent images at times 0, 5, and 10 min of SCMNs loaded with TMRE and incubated with 25 μM mLysoPC + OA for 20 min. The progressive loss of the potentiometric dye TMRE with time indicates a loss of mitochondrial potential. The comparison of the fluorescence images clearly shows a parallel change in mitochondrial shape from elongated to rounded. *Scale bar*, 2 μm. *B*, quantification of the experiment shown in *A*. The loss of fluorescence intensity of five individual mitochondria, expressed as percentages of the initial value, are plotted as a function of time. *Bars*, ±S.D. Similar results were obtained by treatment of CGNs with SPANs.

A loss of TMRE from mitochondria may derive from a decrease of the plasma membrane potential and only a secondary loss of mitochondrial dye without uncoupling (41). This is, however, not the case in the experiment of Fig. 6, because a collapse of plasma membrane potential caused by KCl results in a decrease of the TMRE signal much smaller than that triggered by the lipid mixture (data not shown). The mitochondrial TMRE signal disappears first in the neurite processes and later in the cell body. Fig. 7 clearly shows that the shape of mitochondria is altered as well. It is noteworthy that we noticed an accumulation of mitochondria within bulges (Fig. 7, *panels B* and *C* and *panels E* and *F*). Mitochondria appear swollen and rounded in treated cells, as compared with control neurons imaged by EM (compare *D*, *E*, and *F* of Fig. 7) and fluorescence microscopy (Fig. 7, *G* and *H*).

DISCUSSION

Here, we have documented that SPANs and a lipid mixture composed of LysoPC and OA cause a sustained rise of $[Ca^{2+}]_i$ in nerve terminals with similar time course and extent. This $[Ca^{2+}]_i$ rise mainly derives from the extracellular medium with a little, but significant, contribution from intracellular acidic compartments. Voltage-gated Ca^{2+} channels inhibited by ω-conotoxin MVIIC and nimodipine contribute little, if any, to this Ca^{2+} influx. On the other hand, lysophospholipids have been shown to activate some other types of plasma membrane calcium channels for which there are no specific inhibitors (42, 43) and to cause the formation of transient nonprotein calcium pores in lymphoma cells (37). Whatever the exact pathway of Ca^{2+} entry, a defined role in the intracellular Ca^{2+} rise is also played by a reduced Ca^{2+} efflux, which follows the inhibition of mitochondrial function elicited by SPANs and LysoPC + OA. A number of evidence implicates mitochondria in this reduced Ca^{2+} efflux, including the inability of lipid mixture-treated neurons to bring the increased $[Ca^{2+}]_i$ to resting levels upon EGTA addition (Fig. 5*A*). This is observed even after a few minutes of treatment, when the $[Ca^{2+}]_i$ increase is small (data not shown). Moreover, the shift of intracellular acidic compartments toward neutral pH values after lipid mixture exposure in the absence of extracellular Ca^{2+} (Fig. 3*F*), might be due to a decreased

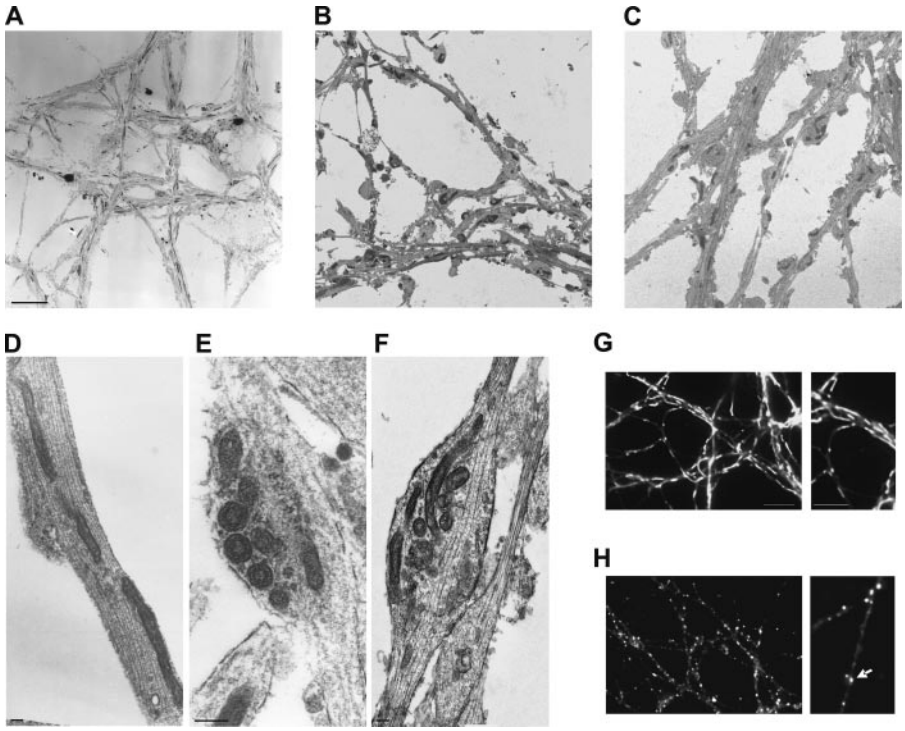

FIGURE 7. **Mitochondria position and morphology are altered by treatment with SPANs and mLysoPC + OA.** *A–F*, transmission EM of control CGNs (*A* and *D*) and of neurons exposed to either taipoxin 6 nM for 1 h (*B* and *E*) or to 25 μM mLysoPC + OA for 15 min (*C* and *F*). *Scale bar*, 2 μm (*A–C*) or 200 nm (*D–F*). Mitochondria accumulate within bulges in both SPAN- and lipid-treated neurons and change shape from elongated (*D*) to condensed (*E* and *F*). Similar behavior was observed in living CGNs loaded with Mitotracker Red (*G* and *H*) in mock-treated (*G*) and mLysoPC + OA-treated samples (*H*; 25 μM for 15 min). High magnification details are shown on the *right*. Similar results were obtained with notexin, β-bungarotoxin, and textilotoxin. *Scale bar*, 2 μm.

ATP level, measured both in living cells using recombinant luciferase (29) or in cell extracts.

Different factors appear to contribute to this mitochondrial impairment: (i) oleic acid and in general fatty acids, which are known to partition into intracellular membranes and to act as mitochondrial uncouplers (33); (ii) an accumulation of Ca^{2+} inside the mitochondrial matrix driven by the electrochemical potential, which is well known to occur as $[Ca^{2+}]_i$ increases and results in mitochondrial damage (44). Taken together, our findings assign a major role to mitochondria damage in the mechanism of SPAN poisoning of nerve terminals and are in agreement with previous *in vitro* studies performed with β-bungarotoxin on synaptosomes (38–40).

Although the morphological and electrophysiological aspects of the paralysis of peripheral nerve terminals caused by SPANs were defined long ago, the underlying molecular mechanisms at the basis of the synaptic inhibition remained unexplained. Recently, we found that the physiological effectors of SPANs are the lipids generated by their hydrolytic activity on membrane phospholipids, which progressively accumulate within the membrane (8). This activity can be mimicked to a large extent by the extracellular addition of an equimolar mixture of LysoPC and fatty acids (8). However, there are intrinsic differences between the action of a SPAN and that of the added lipid mixture that should be recalled here. They derive from SPANs binding to the presynaptic membrane where they display their enzymatic hydrolytic activity. As a result of this SPAN localization, the released LysoPC and fatty acid are well localized within the presynaptic portion of the plasma membrane, at least shortly after SPAN treatment. On the contrary, added lipids have to partition from the water phase into the membrane, and they can do so at any place of the cell surface, included the cell body. This accounts for a less localized calcium increase (compare Figs. 1 and 2). Nonetheless, previous (8) and present data indicate that, whichever read-out we use, snake neurotoxins and lipid mixture addition lead to very similar final results.

Lysophospholipids and FA alter the curvature of the membrane and facilitate exocytosis by promoting the opening of lipidic pores between SV and the plasma membrane. At the same time, they inhibit the reverse process of SV fission (16). The data presented here allow us to complete the picture of events taking place during synaptic intoxication by SPANs. Lysophospholids and FA, released by SPANs, cause a sustained increase of $[Ca^{2+}]_i$ within nerve terminals, which in turn induces the fusion of most SV with the presynaptic membrane. This latter phenomenon has been documented to take place following tetanic stimulation of nerve terminals (22) or latrotoxin treatment (23). This leads to the enlargement of nerve terminals, a feature that establishes one further parallelism between tetanic stimulation and SPAN action, since the tetanized neuromuscular junction is enlarged (22) as well as neurons exposed to SPANs *in vivo* (4) and *in vitro* (8, 9). This analysis strongly strengthens our previous proposal (7, 8) that lysophospholipids and FA, generated by the PLA2 activity of SPANs, are the biochemical effectors of the poisoning action. Moreover, it further supports the notion that the LysoPC + FA mixture is a useful tool for the study and modulation of neuroexocytosis.

Acknowledgments—We thank Prof. P. Bernardi (University of Padova) for help with the assay of mitochondrial membrane potential, S. Gschmeissner (Cancer Research UK EM Unit) for part of the EM analysis. We also thank Prof. R. Deana and Drs. L. Morbiato and A. Zarpellon for help with the measurements of ATP in cell extracts.

REFERENCES

1. Rappuoli, R., and Montecucco, C. (1997) *Protein Toxins and Their Use in Cell Biology*, Oxford University Press, Oxford
2. Kini, R. M. (1997) *Venom Phospholipase A2 Enzymes: Structure, Function, and Mechanism*, John Wiley & Sons, Inc., Chichester, UK
3. Chen, I. L., and Lee, C. Y. (1970) *Virchows Arch. B Cell Pathol.* **6,** 318–325
4. Cull-Candy, S. G., Fohlman, J., Gustavsson, D., Lullmann-Rauch, R., and Thesleff, S. (1976) *Neuroscience* **1,** 175–180
5. Gopalakrishnakone, P., and Hawgood, B. J. (1984) *Toxicon* **22,** 791–804
6. Dixon, R. W., and Harris, J. B. (1999) *Am. J. Pathol.* **154,** 447–455
7. Montecucco, C., and Rossetto, O. (2000) *Trends Biochem. Sci.* **25,** 266–270
8. Rigoni, M., Caccin, P., Gschmeissner, S., Koster, G., Postle, A. D., Rossetto, O., Schiavo, G., and Montecucco, C. (2005) *Science* **310,** 1678–1680
9. Rigoni, M., Schiavo, G., Weston, A. E., Caccin, P., Allegrini, F., Pennuto, M., Valtorta, F., Montecucco, C., and Rossetto, O. (2004) *J. Cell Sci.* **117,** 3561–3570
10. Bonanomi, D., Pennuto, M., Rigoni, M., Rossetto, O., Montecucco, C., and Valtorta, F. (2005) *Mol. Pharmacol.* **67,** 1901–1908
11. Chernomordik, L. V., and Kozlov, M. M. (2003) *Annu. Rev. Biochem.* **72,** 175–207
12. Chernomordik, L. V., and Kozlov, M. M. (2005) *Cell* **123,** 375–382
13. Giraudo, C. G., Hu, C., You, D., Slovic, A. M., Mosharov, E. V., Sulzer, D., Melia, T. J., and Rothman, J. E. (2005) *J. Cell Biol.* **170,** 249–260
14. Xu, Y., Zhang, F., Su, Z., McNew, J. A., and Shin, Y. K. (2005) *Struct. Mol. Biol.* **12,** 417–422
15. Reese, C., and Mayer, A. (2005) *J. Cell Biol.* **171,** 981–990
16. Zimmerberg, J., and Chernomordik, L. V. (2005) *Science* **310,** 1626–1627
17. Corda, D., Colanzi, A., and Luini, A. (2006) *Trends Cell Biol.* **16,** 167–173
18. Murthy, V. N., and De Camilli, P. (2003) *Annu. Rev. Neurosci.* **26,** 701–728
19. Sudhof, T. C. (2004) *Annu. Rev. Neurosci.* **27,** 509–547
20. Ryan, T. A. (2006) *Curr. Opin. Cell Biol.* **18,** 416–421
21. Rizzoli, S. O., and Betz, W. (2005) *Nat. Rev. Neurosci.* **6,** 57–69
22. Ceccarelli, B., Hurlbut, W. P., and Mauro, A. (1972) *J. Cell Biol.* **54,** 30–38
23. Ushkaryov, Y. A., Volynski, K. E., and Ashton, A. C. (2004) *Toxicon* **43,** 527–542
24. Levi, G., Aloisi, F., Ciotti, M. T., and Gallo, V. (1984) *Brain Res.* **290,** 77–86
25. Arce, V., Garces, A., de Bovis, B., Filippi, P., Henderson, C. E., Pettmann, B., and de Lapeyriere, O. (1999) *J. Neurosci. Res.* **55,** 119–126
26. Bohnert, S., and Schiavo, G. (2005) *J. Biol. Chem.* **280,** 42336–42344
27. Giacomello, M., Barbiero, L., Zatti, G., Squitti, R., Binetti, G., Pozzan, T., Fasolato, C., Ghidoni, R., and Pizzo, P. (2005) *Neurobiol. Dis.* **18,** 638–648
28. Bernardi, P., Scorrano, L., Colonna, R., Petronilli, V., and Di Lisa, F. (1999) *Eur. J. Biochem.* **264,** 687–701
29. Jouaville, L. S., Pinton, P., Bastianutto, C., Rutter, G., and Rizzuto, R. (1999). *Proc. Natl. Acad. Sci. U. S. A.* **96,** 13087–13812
30. Rossetto, O., Morbiato, L., Caccin, P., Rigoni, M., and Montecucco, C. (2006) *J. Neurochem.* **97,** 1534–1545
31. Fasolato, C., Zottini, M., Clementi, E., Zacchetti, D., Meldolesi, J., and Pozzan, T. (1991) *J. Biol. Chem.* **266,** 20159–20167
32. Fasolato, C., and Pozzan, T. (1989) *J. Biol. Chem.* **264,** 19630–19636
33. Wojtczak., L., and Schonfeld, P. (1993) *Biochim. Biophys. Acta* **1183,** 41–57
34. Wright, C. E., and Angus, J. A. (1996) *Br. J. Pharmacol.* **119,** 49–56
35. Leung, Y. M., Xion, Y., Ou, Y. J., and Kwan, C. Y. (1998) *Life Sci.* **63,** 965–973

36. Woodley, S. L., Ikenouchi, H., and Barry, W. H. (1991) *J. Mol. Cell Cardiol.* **23,** 671–680
37. Wilson-Asworth, H. A., Judd, A. M., Law, R. M., Freestone, B. D., Taylor, S., Mizukawa, M. K., Cromar, K. R., Sudweeks, S., and Bell, J. D. (2004) *J. Membr. Biol.* **200,** 25–33
38. Ng, R. H., and Howard, B. D. (1978) *Biochemistry* **17,** 4978–4986
39. Nicholls, D., Snelling, R., and Dolly, O. (1985) *Biochem. J.* **229,** 653–662
40. Rugolo, M., Dolly, J. O., and Nicholls, D. G. (1986) *Biochem. J.* **233,** 519–523
41. Rottenberg, H., and Wu, S. (1998) *Biochim. Biophys. Acta.* **1404,** 393–404
42. So, I., Chae, M. R., Kim, S. J., and Lee, S. W. (2005) *Int. J. Impot. Res.* **17,** 475–483
43. Zheng, M., Uchino, T., Kaku, T., Kang, L., Wang, Y., Takebayashi, S., and Ono, K. (2006) *Pharmacology* **76,** 192–200
44. Campanella, M., Pinton, P., and Rizzuto, R. (2004) *Biol. Res.* **37,** 653–660